Journal of Scientific Research & Reports
3(1): 234-254, 2014; Article no. JSRR.2014.012

SCIENCEDOMAIN *international*
www.sciencedomain.org

The Morphology of Naturally Enhanced Ion-acoustic Lines Observed in ESR 42m Data

Bashkim Dalipi[1*]

[1] *University of Prishtina, St. Mother Teresa, 10000, Prishtina, Republic of Kosovo.*

Author's contribution

Author BD, the only author of the paper, has read and approved the final manuscript

Original Research Article

Received 30th June 2013
Accepted 28th September 2013
Published 9th November 2013

ABSTRACT

The Real Time Graph program is capable of generating, as an output, a spectral panel and a power panel, that change in terms of shape and size in response to back-scattered incoherent radar signals. A spectral shape criterion and a power profile criterion are used to evaluate and differentiate between different morphologies for each observed spectra. Analytically, using comparative analysis, four major categories are identified: a normal morphology, a Naturally Enhanced Ion-Acoustic Lines (NEIALs) morphology, a hard object morphology (satellite, space debris, etc.), and a turned-off transmitter morphology. Thirty data dumps are identified as NEIALs, which are investigated in terms of their spectral morphologies and the variations between each type of NEIALs. A "Flambeau"-like spectral shape, along with a "hill"-like power profile, is a distinctive feature of NEIALs. Particular spectra may contain mixed spectral morphologies, such as NEIALs along with hard object(s). NEIALs events may be contained and processed in one single data dump as well in two, three, four, or five consecutive data dumps. The analysis of NEIALs spectral shapes and the corresponding power profiles indicate that the highest intensity of scattered power comes from altitudes between 400 km and 600 km, but most likely about 500 km. We find that the down-shifted ion line shoulder is more often enhanced compared with the up-shifted ion line shoulder. The majority of data dumps show spectral line enhancements that are down-shifted in frequency, while no significant evidence is found for spectral line enhancements that are up-shifted in frequency.

Keywords: Ionosphere; ionospheric physics; incoherent scatter radar; power spectral density.

**Corresponding author: E-mail: bashkimdalipi@gmail.com, bashkim.dalipi@uni-pr.edu;*

1. INTRODUCTION

Naturally enhanced ion-acoustic lines (NEIALs) event have drawn the attention of many authors since the first reported evidence by Foster [1]. Until now, the phenomenon has been treated in the different research reports. There exists a consensus among the authors that the NEIALs are geophysical in their origin.

Different features of NEIALs have been reported in the past. Rietveld [2] showed how the spectra changes from a normal state to a strongly enhanced state and then back again, based on 10 second integrated intervals. The feature of the symmetry and/or asymmetry of shoulder enhancement has been reported in the past by Rietveld [3] based on incoherent UHF radar. Studies on spectral features have been also reported by other authors, for example: Foster [1], Rietveld [2], Collis [4], Forme [5], Wahlund [6], etc. Different features of NEIALs in the domain of statistics have been reported by Rietveld [2] and recently by Ogawa [7]. NEIALs features at high altitudes (1200 - 1900 km) have been reported by Ogawa [8]. In our studies, we investigated the morphology of NEIALs spectra in terms of shape and the size, as shown in a RTG spectral panel.

NEIALs phenomenon, technically contained within the power spectral density, comes as a result of a special investigation technique that is used to study the plasma phenomena in the Earth's ionosphere. This technique is based on incoherent scattering of electromagnetic radiation by the free electrons within the ionospheric plasma. Instruments that enable the implementation of this technique are ground-based with remote-sensing capabilities and are called incoherent scatter radars.

Treating and measuring the total backscattered radiation from the ionosphere, different mathematical roads and approaches have been used. Obtaining the power spectral density equation is, quite complex, and requires deep knowledge about plasma physics and mathematics, and it is beyond the scope of this paper. Therefore, we will present here only the final equation of the power spectral density, e.g. Rosenbluth [9]; Rostoker [10]; Trulsen [11]; Grydeland [12], etc. The total power spectral density is equal to the summation of two partial spectra's, i.e. the electron part, which is a consequence of the electron-acoustic waves, and the ion part, which is a consequence of the ion-acoustic waves:

$$S(\mathbf{k},\omega) = S_{Pline}(\mathbf{k},\omega) + S_{Iline}(\mathbf{k},\omega) \tag{1}$$

$$S(\mathbf{k},\omega) = N_e \left| 1 - \frac{\chi_e(\mathbf{k},\omega)}{\varepsilon(\mathbf{k},\omega)} \right|^2 \int d\mathbf{v}\, f_e(\mathbf{v})\ \delta(\omega - \mathbf{k}\cdot\mathbf{v}) + N_i \left| \frac{\chi_e(\mathbf{k},\omega)}{\varepsilon(\mathbf{k},\omega)} \right|^2 \int d\mathbf{v}\, f_i(\mathbf{v})\ \delta(\omega - \mathbf{k}\cdot\mathbf{v}) \tag{2}$$

$$\chi_\alpha(\mathbf{k},\omega) = \frac{\omega_{pe}^2}{k^2} \int_L \frac{\mathbf{k}\cdot\delta_{\mathbf{v}} f_\alpha(\mathbf{v})}{\omega - \mathbf{k}\cdot\mathbf{v}} d\mathbf{v} \tag{3}$$

$$\varepsilon(\mathbf{k},\omega) = 1 + \sum_\alpha \chi_\alpha(\mathbf{k},\omega) \tag{4}$$

$$\omega_{pe} = \left(\frac{n_e e^2}{m_e \varepsilon_0} \right)^{1/2} \tag{5}$$

Where: k - wave number, $\mathbf{k}$ - wave vector, ω - wave angular frequency, ω_{pe} - electron plasma frequency, , N_e - electron number density, N_i - ion number density, $\chi_\alpha(\mathbf{k},\omega)$ - electric

susceptibility for α species, $f_\alpha(\mathbf{v})$ - velocity distribution function for α species, $\varepsilon(\mathbf{k},\omega)$ - dielectric constant function, $\mathbf{v}$ - electron velocity, n_e - electron density in plasma, e - electron charge, m_e - electron mass, ε_0 - electric permittivity in vacuum and δ - delta function.

The whole spectra (Eq. 1) show two types of spectral lines: the electron-acoustic lines and the ion-acoustic lines (Eq. 2). These lines are the response of two main wave modes known as the ion-acoustic waves and the electron-acoustic waves [13]. The ion-acoustic wave is attenuated, and as a result, the two spectral lines are broadened and in fact, merge to give the characteristic “double-hump” ion spectra [14].

The ion part of the spectra has a characteristic shape, consisting of a two "shoulders" double-peaked shape (see Fig. 1) and is partly overlapped [15]. The ion lines are the central part of the spectra, typically extending over several kHz around the radar transmitter frequency [16]. The up-shifted shoulder corresponds to an ion-acoustic wave (IAW) propagating towards the receiving antenna, while the down-shifted shoulder corresponds to an IAW propagating away from the receiving antenna [17]. The electron part lies on both sides of the beam emitting radar frequency, but at a distance of ($\pm$) a few hundreds of kHz away from the radar frequency.

Even though the physical basis of the incoherent scatter technique is Thompson scattering, the essential role in determining the shape and the size of the power spectral density is played by the density fluctuation of the plasma. Some recent studies consider the formation of a gap in the spatial power spectrum and evaluation of its double-humped shape of electron density fluctuations in plasma at different angle of inclination of prolate irregularities with respect to external magnetic field [18],[19].

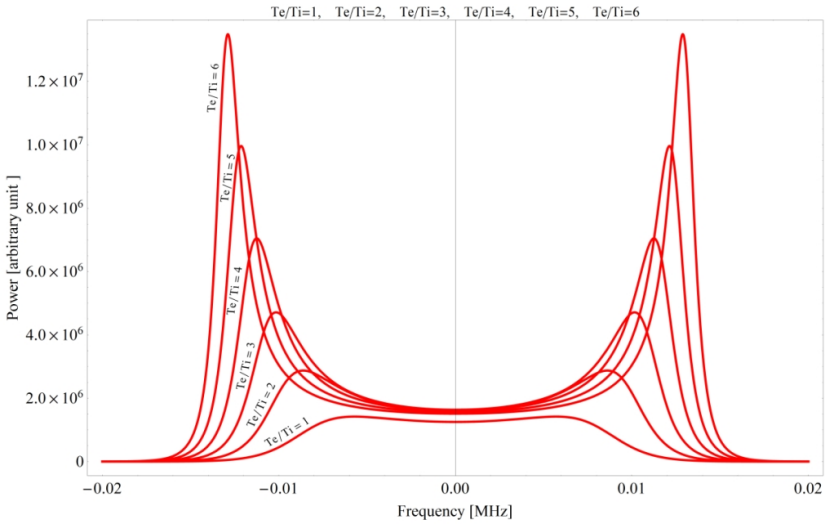

Fig. 1. Theoretical form of the ion lines. The down-shifted and the up-shifted ion line shoulders. The shape of the ion line is governed by plasma properties in the ionosphere. The shape is very sensitive to the changes of Te/Ti ratio. Our examples show the shape for cases: Te/Ti=1, Te/Ti=2, Te/Ti=3 Te/Ti=4, Te/Ti=5 and Te/Ti=6 [20].

The spectral shape of the power spectral density is very sensitive and in a close relationship with the ionospheric plasma parameter fluctuations. Fig. 1 shows the relationship between

the electron to ion temperature ratio (Te/Ti) and the corresponding shape of the spectra considering Maxwellian plasma conditions [20].

Namely, two main ionospheric plasma conditions are to be considered: Maxwellian plasma and non-Maxwellian plasma. At the Maxwellian plasma, the ion lines of power spectral density shows a good symmetry between the "shoulders", while at the non-Maxwellian plasma, the main characteristic feature is the enhancement and/or the asymmetry between the "shoulders". The features of the power spectral density are the subject of our investigation in terms of the spectral morphology enabled by a Real Time Graph (RTG) program.

2. MATERIALS AND METHODS

There are several radar facilities worldwide that are using the incoherent scatter technique to study the ionosphere and the upper atmosphere. One of them is the EISCAT radar facility (European Incoherent Scatter Scientific Association). An extension of the EISCAT radar facility is the EISCAT Svalbard Radar (ESR) system, which consists of two antennas (ESR 42m and ESR 32m), and it's a very advanced radar system. The ESR 42m antenna is fixed and field-aligned, while the ESR 32m antenna is fully steerable. It is movable 360^0 in azimuth and 0^0 to 180^0 in elevation. The EISCAT Svalbard Radar system operates at a frequency of 500 MHz. Geographically, the radars are positioned at the following coordinates: $78^0\ 09'\ 11''\ \mathrm{N}$ and $16^0\ 01'\ 44''\ \mathrm{E}$.

The ESR runs three kinds of programmes: Common Programmes (CP), Special Programmes (SP) and Other Programmes. In our study, we have used the first general-purpose ESR experiment **tau0** (6.4 second per dump) which covers all altitudes from 70 km to over 1200 km. The ESR output data were stored as raw matlab files (6.4 s dump) which can be Fourier transformed into spectra using the Real Time Graph (RTG) program. Our used data were produced during 10.64 hours of atmosphere scans on 01 June 2004 from a CP program schedule using the ESR 42m antenna. The source of data was EISCAT data archive. Using the TAPECAT and get_mat command, we were able to separate a group of data sets representing continuous scans of the atmosphere on 01 June 2004.

To display the power spectral density, we used a Matlab based program called Real Time Graph, version 2.6, and an appropriate definition file called rtg_tau0_510.m. RTG, with such a definition file, has the capability to display a spectral panel (Fig. 2) and another panel that graphs the power returns from the ionosphere.

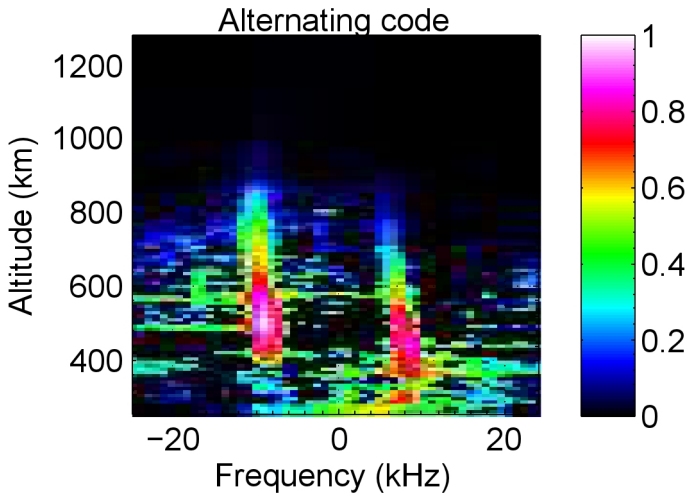

Fig. 2. An example of the spectra panel, which is capable of visualizing the NEIALs during an integration time of 6.4 s using the RTG program, and the definition file rtg_tau0_510.m.

3. RESULTS AND DISCUSSION

Analytically, using comparative analysis, we have made the distinction between four major morphological features of the spectra (i.e. the shapes and the sizes) as follows: the normal morphology, NEIALs morphology, the hard object morphology, and the spectra output recorded by the antenna receiver when the transmitter is turned-off (transmitter-off morphology).

We have based the distinction between different spectral morphologies on two rigid criteria. The first criterion consists of the behavior of the power profile (i.e altitude profile of returned power) for each data dump transition. The spectra where the corresponding power profile firmly and steadily overlaps from dump to dump (i.e. no significant power profile deviation compared to the previous dump) are classified as normal spectra. The altitude profiles of returned power of normal spectra forms a "ski-jump-hill"-like power profile. The altitude profile of returned power that during dump transition makes a change from a common "ski-jump-hill"-like power profile, either slightly or considerably, and which at a particular altitude forms a "hill"-like power profile, are classified as NEIALs. The altitude profile of returned power that at a particular altitude sharply mounts up and forms a "boxcar"-like power profile is classified as a hard object. Finally, in the case where the altitude profile of returned power forms a "zigzag"-like power profile around zero, the value indicates that the transmission or the transmitter/radar is turned-off.

Indeed, the power-returns that come from a very limited altitude range are assumed to be scattering from a hard target, such as a satellite, but when these large returns are extended in altitude along the geomagnetic field, they are assumed to be of geophysical origin [21]. It is suspected that many of the hard object cases found are due to satellites or space debris passing through the main beam or the side lobes [22].

The second criterion for making the distinction between the four major spectral morphologies is based on spectral panel shapes. If there is shown a "double-humped"-like shape of the spectra (corresponding up-shifted, respectively down-shifted ion line), such a case is classified as a normal spectra. If the area of the spectra is filled out with one or two "Flambeau"-like shapes (a flaming torch shape of RTG spectral image, like the one shown in figure Fig. 2), representing down-shifted or up-shifted shoulder enhancement, these spectra are classified as NEIALs. A hard object spectral shape represents a disturbance, stretching horizontally according to the scattering height, but it's also very common that twinkling spots structures can associate with such objects. Object spectra, in general, have a "lens-flare"-like shape. And finally, a "noise-on-screen"-like spectral shape is a spectral characteristic when the transmitter is turned-off.

So a "double-humped"-like spectral shape along with a "ski-jump-hill"-like power profile is assigned for a normal spectra; A "Flambeau"-like spectral shape along with a "hill"-like power profile is assigned for a NEIAL; a "lens-flare"-like spectral shape along a with "boxcar"-like power profile is assigned for a hard object; and finally, "noise-on-screen"-like spectral shape along with a "zigzag"-like power profile is assigned for a spectra recorded when there is no transmission (Fig. 3).

Additionally, the data dumps containing NEIALs are grouped in sequences. A sequence represents a group of data dumps which in their spectra consecutively contain NEIALs morphology. A sequence is assumed to present an individual NEIALs event. These events, depending on the maximum of power recorded, are classified in three groups: (1) a weak process - if the peak of power varies between 0K to 100K; (2) a moderate process - if the peak of power varies between 100K and 1000K; and (3) a strong process - if the peak of power varies between 1000K and the infinite.

Using our criteria, we found that during our observational time interval, a totally of 5141 6.4-second data dumps, covering an interval of time equal to 9.4 hours, were shown with spectra either normal, NEIALs, or hard object morphology. The time remaining, equal to 1.5 hours, represents the transmitter turned-off and this interval of time is discretely distributed in different time intervals.

The first data dump containing NEIALs was found at 07:31:08 UT and the last one at 11:59:18 UT. No NEIALs were found after 11:59:18 UT until the last data dump was observed, i.e. 18:01:07 UT. In total we found 30 data dumps, which contained NEIALs to some extent.

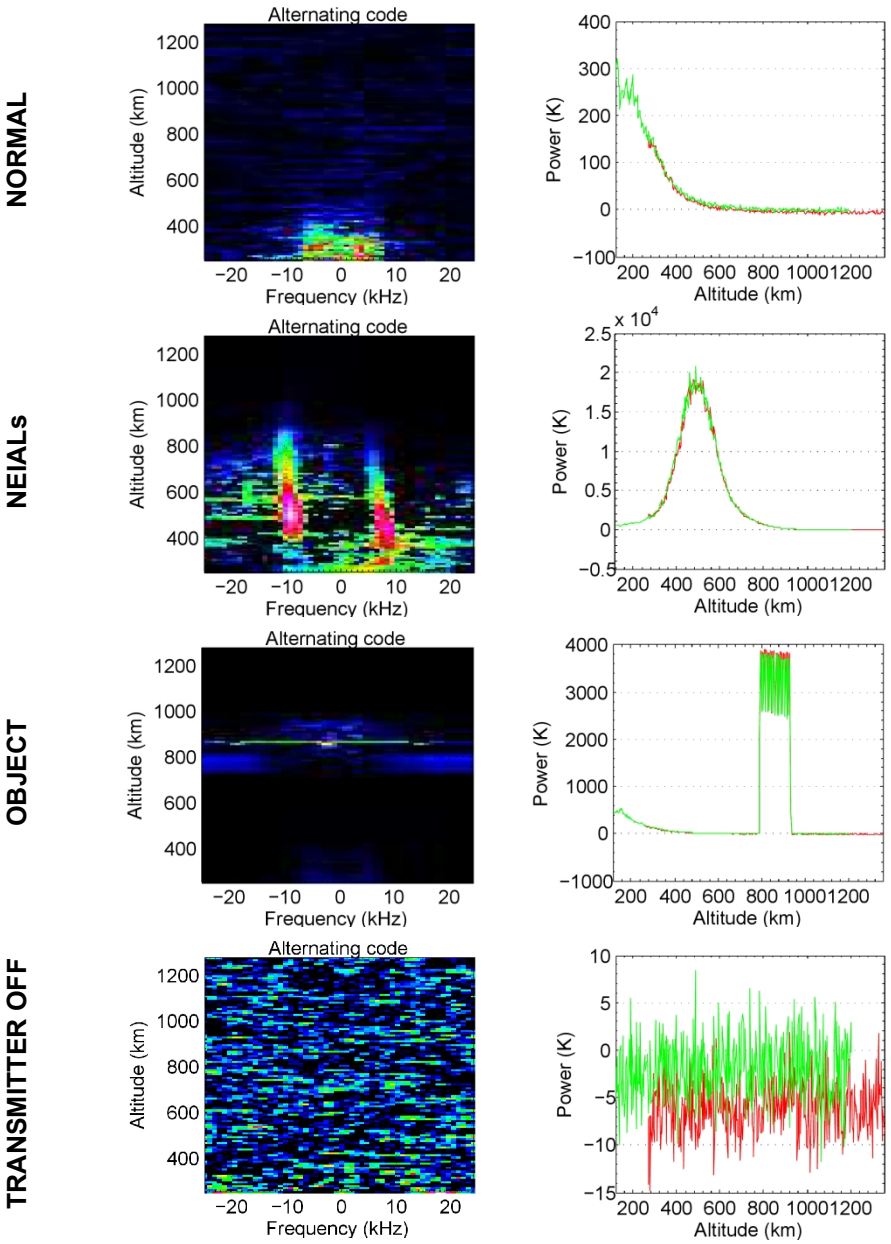

Fig. 3. Distinctions between the four major morphological features of the spectra: Four different outputs for four different data dumps. The power profile graph between a NEIALs event and a hard object event is clearly different. A "hill"-like altitude profile of returned power for NEIALs against a "boxcar"-like power profile for a hard target and a "zigzag"-like power profile around the zero value for recording with the transmitter turned-off. A "Flambeau"-like spectral shape shown in a RTG spectral panel is another distinction feature for NEIALs.

These data dumps were classified as sequences of one, two, three, four and five consecutive dumps. Preceding and successive data dumps of every sequence typically

shows the normal spectral morphology, while inside the sequence, the spectra changes from normal to NEIALs and back again [2].

From the total number of data dumps observed, evaluated as NEIALs (Fig. 4 to Fig. 14), only in two cases did a NEIALs process develop within one individual data dump (07:43:05 UT and 08:03:15 UT). In two other cases, the NEIALs process developed consecutively in two data dumps (07:36:41-07:36:48 UT; 08:03:47-08:03:53 UT). In one case, the NEIALs developed in three consecutive data dumps (11:59:12-11:59:24 UT). In four cases, NEIALs processes developed in four consecutive data dumps (07:31:08-07:31:27 UT; 07:35:56-07:36:16 UT; 08:07:44-08:08:03 UT; 08:16:09-08:16:28 UT). And finally, in one case, the NEIALs process developed in five consecutive data dumps (08:19:27 UT to 08:19:53 UT).

In the following, we investigated the spectral morphology of selected data dumps in order to observe NEIALs and study the morphological behavior of such a spectra among the selected dumps.

Event one: The first encountered spectra, with slightly enhanced shoulders, were those ranked consecutively from 07:31:08 UT to 07:31:27 UT (Fig. 4). The morphology of the spectra varied gently from dump to dump. The variation is noticed more in the spectral shape terms than in the power profile terms. Within the first dump (07:31:04 UT), the spectra showed a very weak enhancement in the down-shifted shoulder, which was intensified slightly in the second dump (07:31:15 UT). In the third data dump (07:31:21 UT), the spectra almost passed through the normal shape, while in the fourth data dump, a very slight enhancement was observed in the down-shifted shoulder. All together, these four spectra may represent a single event that lasted for a maximum of 4 x 6.4 seconds, i.e. 25.6 seconds.

Every data dump, composing the sequence one, shows almost a "ski-jump-hill"-like power profile. Therefore, in terms of the power profile, there is no solid evidence to support unequivocally the existence of NEIALs. However, in terms of spectral shape, the evidence is lightly prominent. Therefore, we have chosen to classify this event as a weak process of NEIALs.

The fact that the third spectra passes through a normal morphology (i.e. almost no enhancement is present), may indicate that there is more than one independent event in play. Moreover, since the shape of the spectra, for one single data dump, in fact, represents the overall summation of the power for 6.4 seconds, it's quite difficult to define whether the NEIALs represent a single correlated event or two or more uncorrelated events. If we assume only one correlated event, this is likely one event that would correspond to an auroral structure moving into and out of the radar beam. High-resolution measurements can be used to follow the development of the enhancements as a function of altitude and time [23]. Overall, this event (event one) could be classified as a weak process of NEIALs.

Event two: Within a time domain of four consecutive data dumps, from 07:35:56 UT to 07:36:16 UT (Fig. 5), four different spectra with different spectral morphologies were observed. Based on our criteria, each one was classified as NEIALs contained. In this sequence, the "Flambeau"-like spectral shape along with a "hill"-like power profile was very notable, especially at the second and at the third dump.

The first dump (07:35:56 UT) showed an up-shifted shoulder enhancement that extended between an altitude of 400 km and 600 km. The maximum of the power intensity was integrated at an altitude of 450 km. Within the altitude extension of spectral enhancement,

the up-shifted shoulder of the ion line also showed extension pretty much over the frequency range. The power graph reached its maximum at around 380 K.

The successor data dump (07:36:03 UT) showed a transition of the domination between the shoulders, from the up-shifted one to the down-shifted one. Enhancement in the down-shifted reached its maximum at an altitude of about 470 km and the frequency of -9 kHz, while in the up-shifted one, the maximum was integrated at an altitude of around 470 km and the frequency of about 7.5 kHz. It is evident that the enhancements in both spectral lines were down-shifted in frequency, and was consistent with ion outflow [24]. In the actual spectra, the altitude extension of the down-shifted shoulder covered an altitude range of about 500 km.

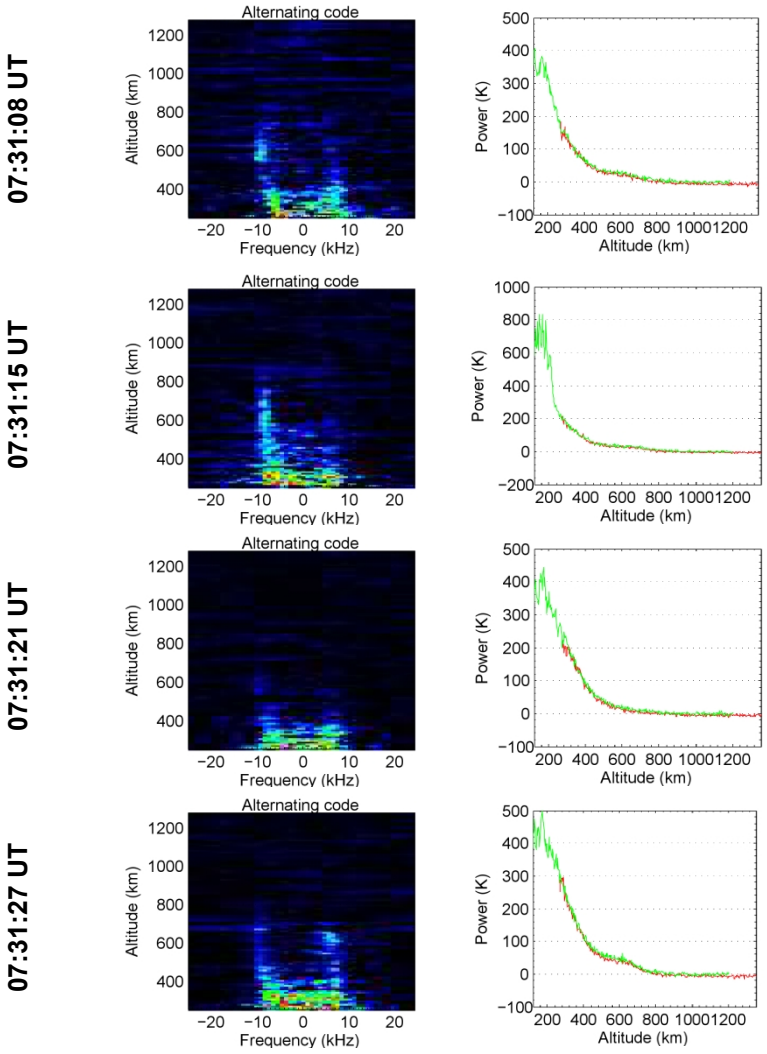

Fig. 4. Event one: Development of a weak process of NEIALs in 4 consecutive data dumps. The process was dumped at 07:31:08 UT and continued until 07:31:27 UT. In the third data dump (07:31:21 UT) the spectra almost passed through a normal morphology, while in the last dump, a little tendency for a down-shifted shoulder enhancement was evident.

In the third data dump (07:36:09 UT) the spectral enhancement achieved its maximum in terms of the power returned. The maximum power registered was about 19000 K. The intensity peak for the down-shifted shoulder was positioned at around 510 km, while for the up-shifted shoulder was positioned at around 440 km. In Fig. 5, we could clearly see an altitude difference for the maximum intensity between the down-shifted and the up-shifted shoulder. This difference was about 70 km. As in the previous data dump, it was evident that the enhancements in both spectral lines were down-shifted in frequency. The surface area of the spectral panel was significantly colorized that showed us very much ion line disturbance during that interval of time.

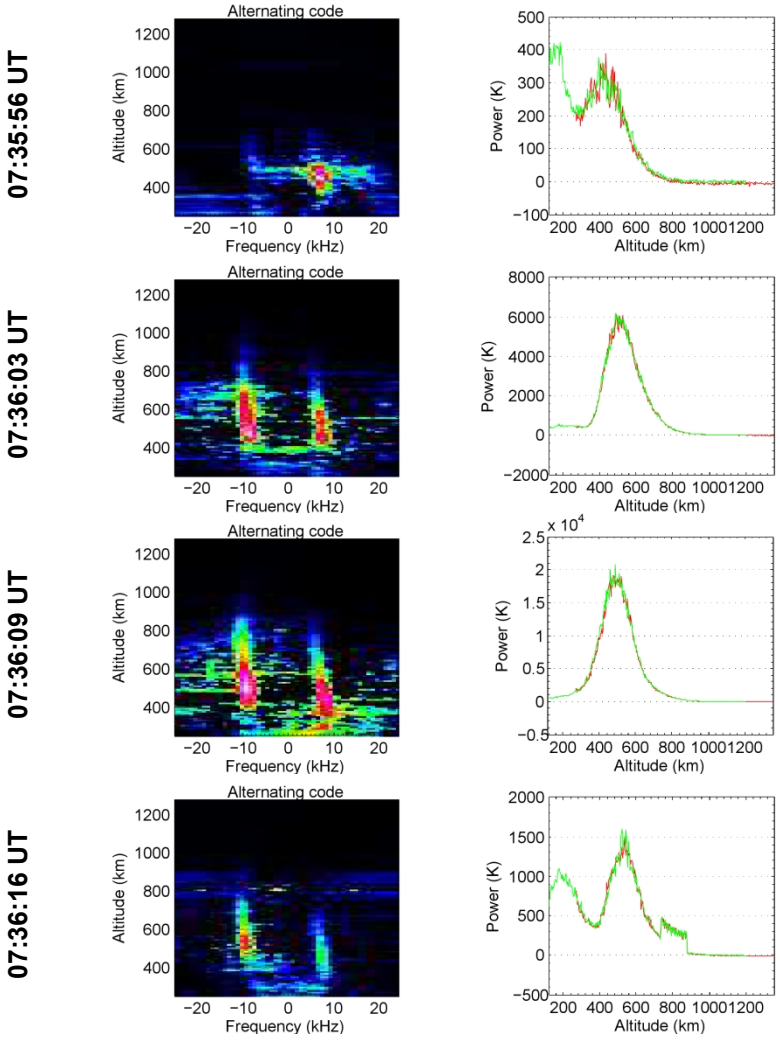

Fig. 5. Event two. Development of a strong process of NEIALs in four consecutive data dumps. Initially, the process was dumped at 07:35:56 UT. In the third data dump the power reached its maximum, about 19000 K. At this dump the "Flambeau"-like spectral shape was very much emphasized in the down-shifted shoulder. The last data dump signed by NEIALs was at 07:36:16 UT. The power profile for this dump contained a "hill"-like power profile along with a "boxcar"-like power profile.

This was likely an artifact of the Fast Fourier Transform process on the signal with strong peaks and did not represent real power spread out so much in frequency and altitude. The altitude extension for the down-shifted and up-shifted shoulder remained approximately the same as in the previous dump.

In the last data dump (07:36:16 UT), for this event, we saw the tendency of the spectral stabilization to a normal morphology, but still with the premises of enhanced ion lines, which were more notable in the down-shifted shoulder. The power decreased over ten times more than in the previous dump. The power profile for this data dump also contained, among a "hill"-like power profile, a "boxcar"-like power profile, positioned at altitude at around 800 km. It means that the spectra contained a hard object power return among the NEIALs. The successor data dump (figure for that data dump is not shown) showed a very typical shape of the spectra that we call a normal spectra, with only insignificant power return from a hard target and twinkling spots at an altitude of about 800 km.

Judging from the continuity of the event from dump to dump, we may conclude that this sequence presented a major plasma event that developed in time, and in space and which lasted for a maximum of 25.6 seconds. Based on our criteria, this event (event two) could be classified as a strong process of NEIALs.

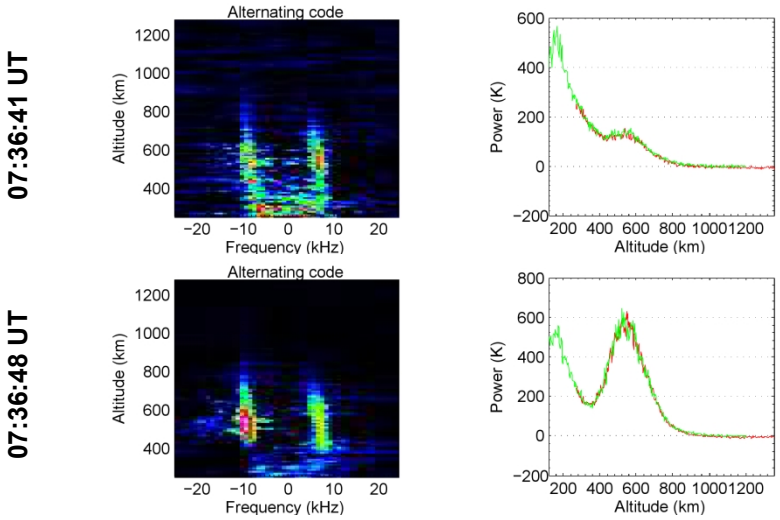

Fig. 6. Event three: Development of a moderate process of NEIALs in two consecutive data dumps. The process was dumped consecutively at 07:36:41 UT and at 07:36:48 UT.

Event three: The subsequent event happened inside a sequence of two consecutive data dumps, and developed at 07:36:41 UT and at 07:36:48 UT (Fig. 6). In the first data dump (07:36:41 UT), the power graph showed a "hill"-like power profile with a power peak of 130 K at an altitude of about 600 km. Both shoulders were approximately equally enhanced, and the enhancements in both shoulders were down-shifted in frequency. The ion line enhancements were seen within an altitude extension between 400 km and 700 km for both shoulders.

At the second data dump (07:36:48 UT), the power graph showed, without a doubt, a "hill"-like power profile together with a "Flambeau"-like spectral shape, which was more notable in the down-shifted shoulder. The peak of the power profile reached up to 650 K. The altitude extension for the ion line enhancement remained the same as in the precede data dump. However, the down-shifted shoulder was more enhanced and showed higher intensity than the up-shifted one. The maximum of the enhancement in the down-shifted shoulder was integrated at an altitude of about 510 km. Also, the enhancements in both shoulders remained down-shifted in frequency about the same as in the previous dump. Based on our criteria, this event (event three) could be classified as a moderate process of NEIALs.

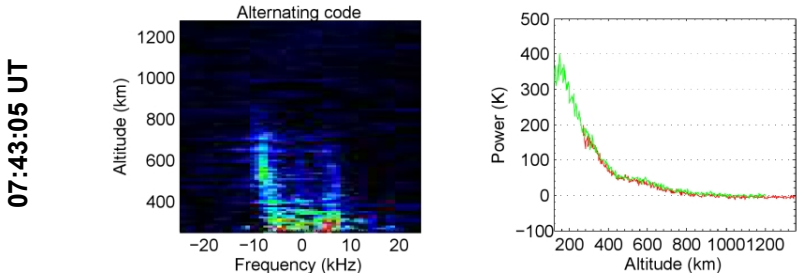

Fig. 7. Event four: Development of a weak process of NEIALs in a single data dump (07:43:05 UT). The down-shifted shoulder ion lines were more enhanced, and more altitude extended.

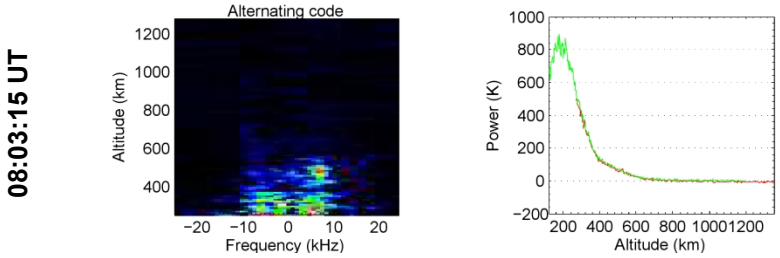

Fig. 8. Event five: Development of a weak process of NEIALs in a single data dump (08:03:15 UT). The power profile and the spectral shape were very close to the normal one.

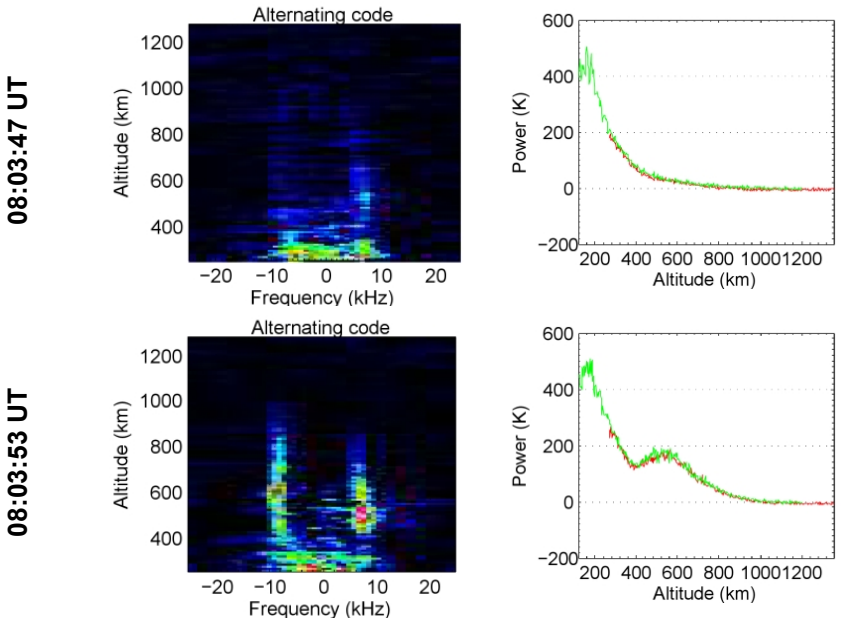

Fig. 9. Event six: Development of a moderate NEIALs process in two consecutive data dumps, starting at 08:03:47 UT and ending at 08:03:53 UT.

Event four and event five: The next two coming events that we faced during our observation were those at the time 07:43:05 UT and 08:03:15 UT (Fig. 7 and Fig. 8). These dumps were classified as being standalone, and containing NEIALs events. In terms of power profile, there was almost no power increase compared to what we faced at the power profile for normal spectra, but in terms of the spectral panel shape, a weak down-shifted shoulder enhancement at 07:43:05 UT and a weak up-shifted shoulder enhancement at 08:03:15 UT was evident. Even though we classified the dump at 08:03:15 UT as NEIALs contained, our accuracy of judgment lies somewhere between being NEIALs to being normal spectra. Both events could be classified as weak processes of NEIALs.

Event six: The next NEIALs event was contained in two consecutive dumps, at 08:03:47 UT and at 08:03:53 UT (Fig. 9). In the spectral shape of the first data dump the NEIALs were barely seen, but in the upcoming dump it was more prominent in the spectra and, also, in the power profile. The power reached around 180 K.

The enhancements were centered in frequency in both shoulders. In the second dump, the maximum of the enhancement intensity in the down-shifted shoulder was positioned at an altitude of about 615 km, while in the up-shifted shoulder at about 500 km. In this dump, the ion line asymmetry was dominated all through the altitude extension. Event six could be classified as a moderate process of NEIALs.

Event seven: Another NEIALs event, occurring among a time interval of 4 x 6.4 seconds is contained in a sequence of four consecutive data dumps (08:07:44 UT to 08:08:03 UT, Fig. 10).

At the first data dump of this sequence (08:07:44 UT), we saw weak ion line enhancements in the down-shifted shoulder which extended up to 1100 km in altitude, while the up-shifted

shoulder did not contain prominent enhancement. At the second dump (08:07:50 UT) the enhancement shifted a bit to the up-shifted shoulder. The power profile almost did not change its routine at all.

At the third dump (08:07:56 UT), the area of the spectra was clearly filled with two "Flambeau"-like shapes, corresponding to the down-shifted and the up-shifted ion line enhancements. The power graph had a "hill"-like power profile. In this case, surely we were dealing with the intensified up-shifted NEIALs that extended from about 400 km up to 850 km. In the other side, the altitude extension for the enhanced down-shifted shoulder varied between 400 km to about 1000 km. The power intensity scattered from the ionosphere exceeded 1000 K. The peak of the enhancement intensity for the up-shifted shoulder is found to be at about 460 km. The down-shifted shoulder was slightly less enhanced than the up-shifted shoulder. As in the second event, both of "Flambeau"-like shapes were down-shifted in frequency.

At the fourth dump (08:08:03 UT), the area of the spectra was considerably colorized. The power profile showed high values of the power returned from the ionosphere which was over 5000 K. The majorities of NEIALs were contained at the down-shifted shoulder and considerably dominated the up-shifted shoulder. The altitude extension of the enhancements for both shoulders had not changed substantially, compared to the preceding data dump. However, the frequency extension for the down-shifted shoulder was significantly increased compared to the preceding dump. So, it is clear that NEIALs were very much disturbed over the frequency range. As we went through this sequence, one can see that the maximum of the plasma process was dumped at the last data dump. A “Flambeau”- like shape was very much emphasized in the down-shifted shoulder. Based on our criteria, this event could be classified as a strong process of NEIALs.

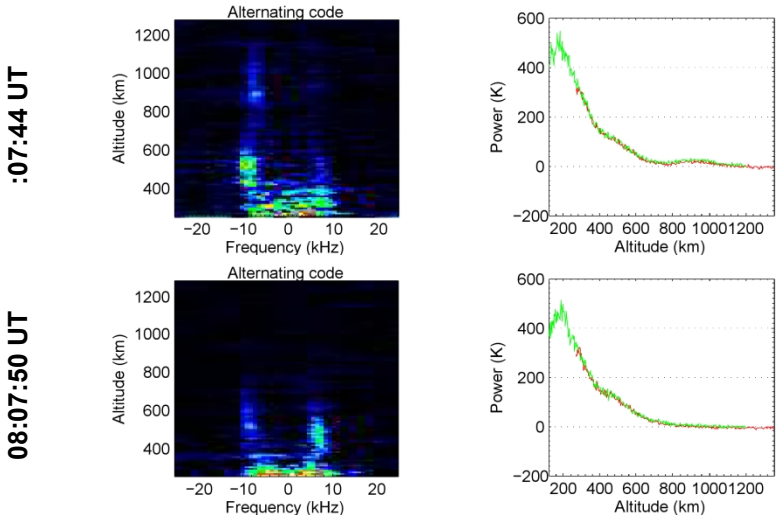

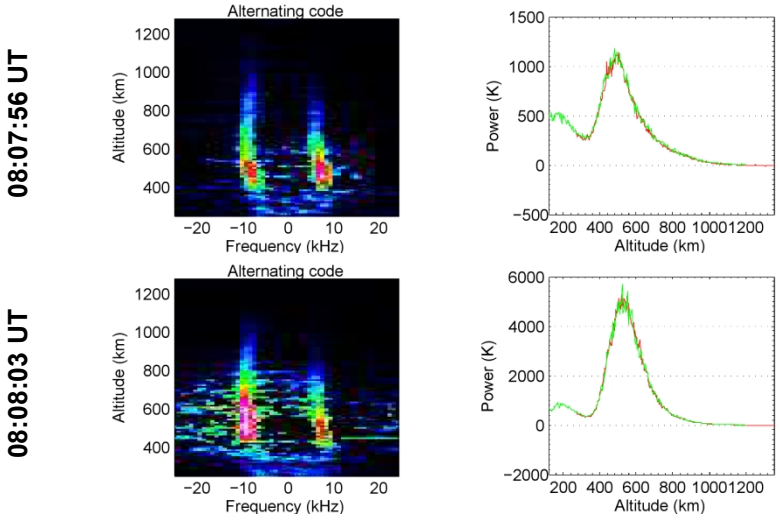

Fig. 10. Event seven: Development of a strong process of NEIALs in four consecutive data dumps. In the fourth data dump (08:08:03 UT) the power reaches its maximum, over 5000 K.

Event eight: The upcoming NEIALs event lay within a sequence composed by four consecutive data dumps (08:16:09 UT to 08:16:28 UT, Fig. 11). In the first spectra, we noticed ion line enhancements only in the up-shifted shoulder, while the second spectra showed enhancements of both shoulders. In the third spectra, a "Flambeau"-like shape was emphasized in the down-shifted shoulder and a "hill"-like power profile was clear. The majority of the ion line enhancement for the down-shifted and the up-shifted shoulder was positioned at around 500 km. The altitude extension for the down-shifted shoulder was about two times greater than for the up-shifted shoulder. In the last data dump for this sequence, the spectra reset almost to a normal morphology. This event could be classified as a strong process of NEIALs, considering that the maximum of the power returned, in the third data dump, is about 1400 K.

Event nine: This was the longest sequence we found, and it was composed by five consecutive data dumps (08:19:27 UT to 08:19:53 UT, Fig. 12). The power profiles for these five consecutive data dumps showed no significant change compared to the power profiles that came from the data dumps showing containing normal spectral morphologies. However, in the second data dump (08:19:34 UT), we could see a visible "hill"-like power profile mounted in the power graph. The maximum of the enhancement intensity in the up-shifted shoulder was positioned at an altitude of about 200 km.

Based on our criteria, this event could be classified as a moderate process of NEIALs, considering that the maximum of the power returned, in the second data dump, is about 200 K. Overall, in terms of the spectral morphologies, the distinction between the data dumps was more clearly notable than it was in power profile terms.

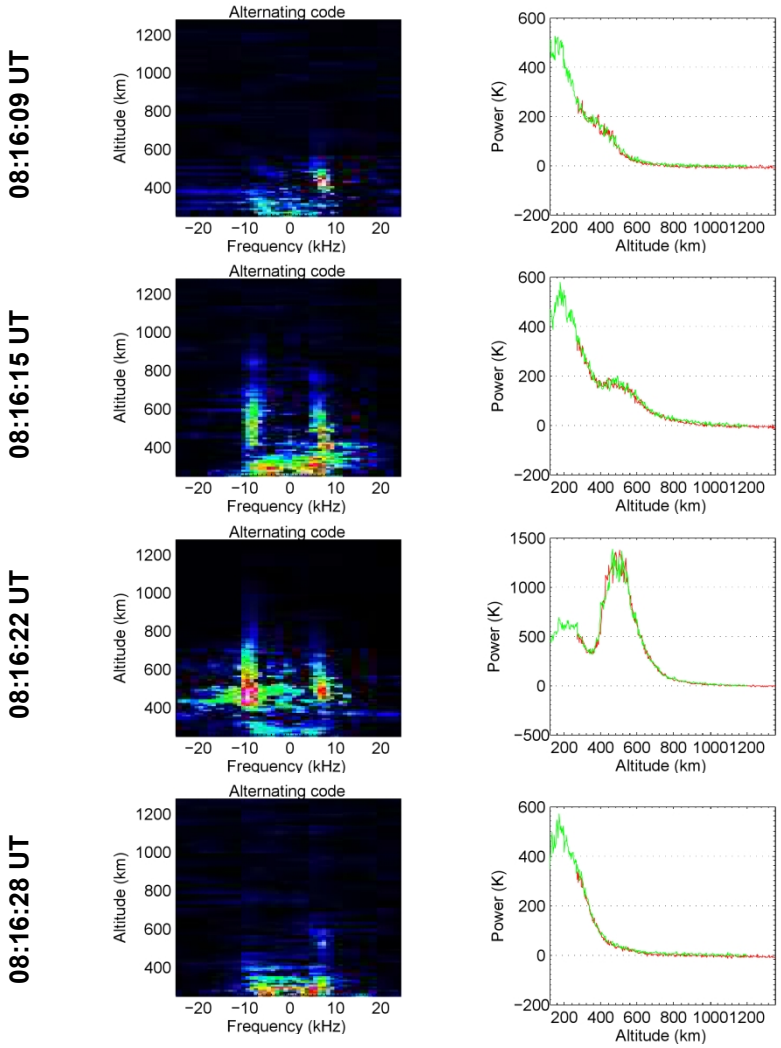

Fig. 11. Event eight: Development of a strong process of NEIALs in four consecutive data dumps. In the third data dump (08:16:22 UT), the power reached its maximum, around 1400 K.

Event Ten: The last sequence of NEIALs event was developed close to noontime (11:59:12 UT to 11:59:24 UT, Fig. 13). At 11:59:12 UT, the power graph showed an increase of power scattered at an altitude of about 510 km. The spectral panel showed an increase of the colorized area below 600 km for both shoulders. The ion lines were exaggerated in the frequency domain, especially in the up-shifted shoulder, where the "Flambeau"-like morphology was dominant.

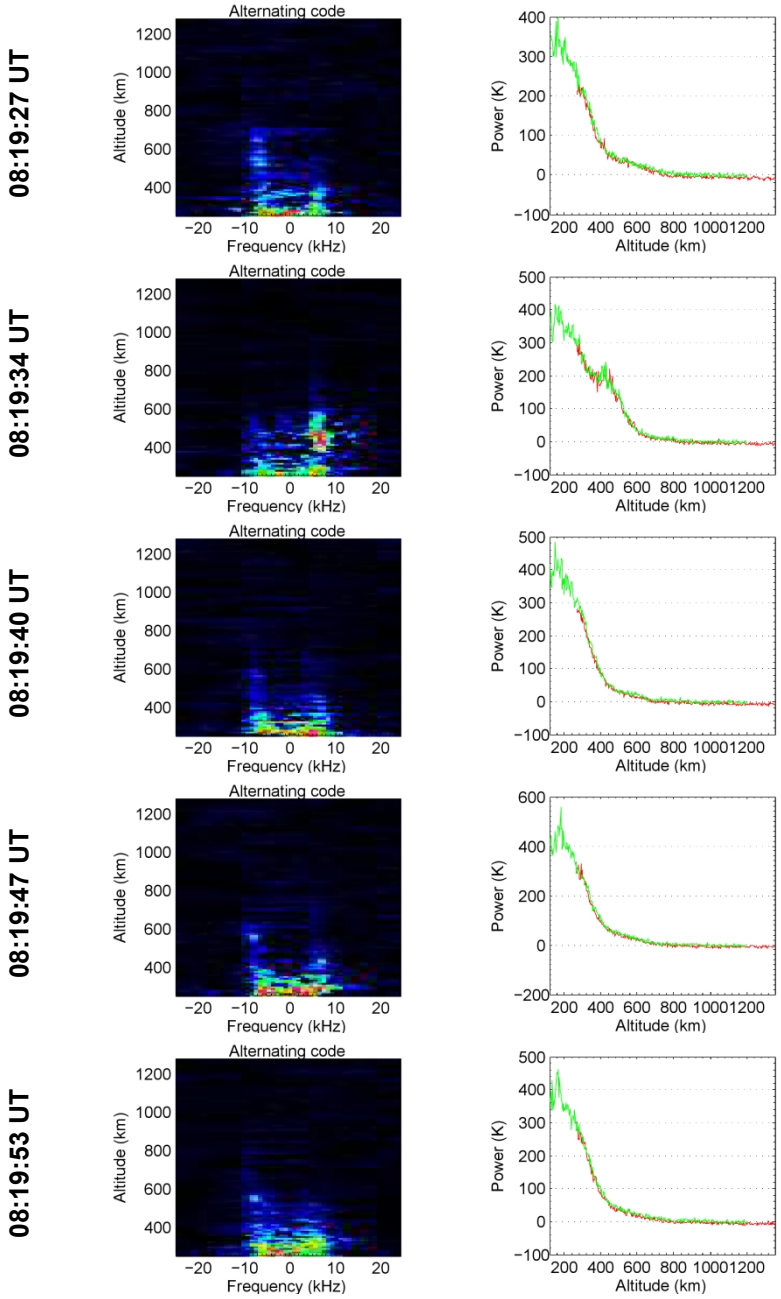

Fig. 12. Event nine: Development of a weak process of NEIALs in five consecutive raw data dumps. The process was dumped, a bit more significantly, only in the second data dump (08:19:34 UT).

At 11:59:18 UT, the process reached its maximum. We clearly saw a shift of NEIALs dominance from the up-shifted shoulder to the down-shifted shoulder, during the dump transition. The down-shifted ion lines were very much exaggerated in the frequency domain. The maximum of the power returned came from an altitude of about 410km. This was the

lowest altitude height, we found, that represented the maximum intensity of the ion line enhancement coming from such a low altitude height. The last dump (11:59:24 UT) showed the normalization of the spectral morphology with very little content of NEIALs. This event could be classified as a strong process of NEIALs, considering that the maximum of the power returned, in the second data dump, is about 1900 K.

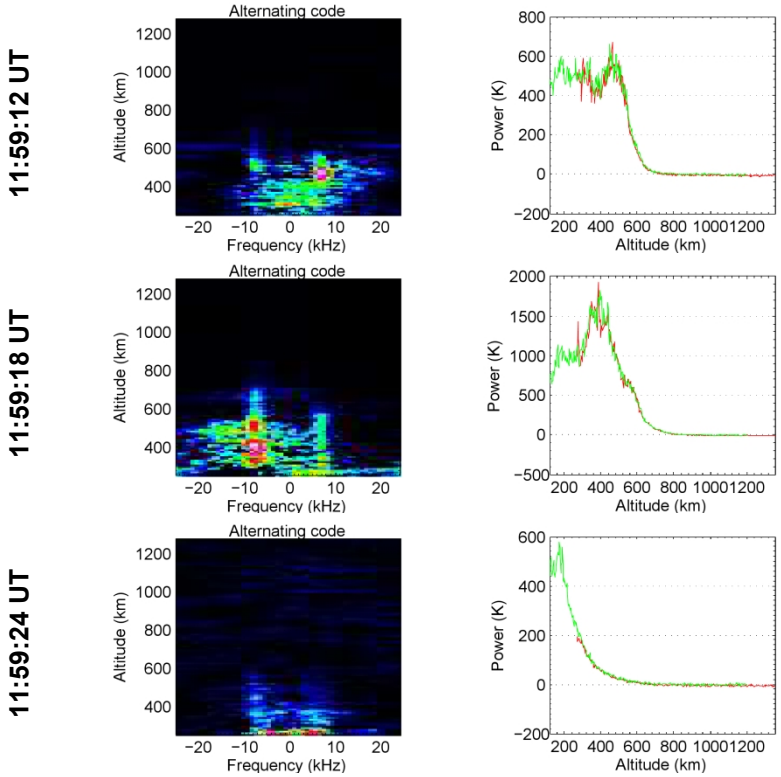

Fig. 13. Event ten: Development of a strong process of NEIALs in three consecutive data dumps. In the second data dump (11:59:18 UT), the power reached its maximum, around 1900 K. Within the second dump, the down-shifted ion lines are much more emphasized compared to the up-shifted ion lines.

Comparing and contrasting the spectral morphologies of all analyzed data dumps, containing NEIALs, in terms of occurrence frequency of up-shifted or down-shifted shoulder enhancement, we found the following statistics: In 17 out of 30 observed NEIALs, the down-shifted shoulder enhancement dominated the statistics, while in 13 out of 30 discovered NEIALs; the up-shifted shoulder enhancement dominated the statistics.

In general, the down-shifted ion line shoulder was more often enhanced compared to the up-shifted ion line shoulder.

In terms of the whole spectral shift, the statistics were dominated by the down-shifted ion lines. The majority of the observed data dumps contained the ion line shoulder enhancements which are down-shifted in frequency, more or less, indicating upward ion

motion. There was no significant evidence for whole spectral shoulder enhancements, which are up-shifted in frequency.

4. CONCLUSION

The incoherent scatter power spectral density, enabled by a RTG program, as a spectral panel along with a power panel, is a very powerful and suitable tool for monitoring the morphological changes in the spectra for each sampled data dump.

Analytically, using comparative analysis based on the shape and the size, four major categories are identified: the normal morphology, naturally enhanced ion-acoustic lines morphology (NEIALs), the hard object morphology (satellite, space debris, etc.), and the transmitter turned-off morphology.

A "Flambeau"-like spectral shape, along with a "hill"-like power profile, is a distinctive feature of NEIALs, and a "lens-flare"-like spectral shape, along with "boxcar"-like power profile, is a distinctive feature of a hard object.

We have observed different spectral morphologies for different short-lasting or long-lasting NEIALs events. The best noticeable case was that of event two, and the least noticeable was that of event four.

Looking at different classified NEIALs sequences and at each constitutive data dump morphology, and considering the continuity of "Flambeau"-like spectral shape along with a "hill"-like power profile that occurred from dump to dump, it's intuitive and analytic and may lead us to the conclusion that most of the NEIALs events observed were, more or less, correlated processes and developed in time scales exceeding 6.4 s. The plasma processes associated with NEIALs, in most cases were carried out in more than one single data dump. However, such events surely can also last for a shorter period of time, less than 6.4 s. This was demonstrated in our observed event four and event five. Therefore, NEIALs processes can last less than 6.4 seconds up to several times more than 6.4 seconds.

The analysis of NEIALs spectral shapes and the corresponding power profiles indicates that the highest intensity of scattered power comes from the altitudes between 400 km to 600 km but most likely around 500 km.

We also conclude that a single data dump may contain mixed morphologies. During our observations, we found cases where signatures exist for both NEIALs and hard objects in the same data dump.

Comparing and contrasting the analyzed data dumps, containing NEIALs, we can conclude that the down-shifted ion line shoulder enhancement dominates the statistics against the up-shifted ion line shoulder. Also we can conclude that the majority of data dumps showed the spectral line enhancements which were down-shifted in frequency, while no significant evidence was found for the spectral line enhancements which were up-shifted in frequency.

For further work, we suggest observing larger sets of raw data in order to more comprehensively map the synoptic of data dump spectral morphology that could indirectly indicate the synoptic of the Earth’s ionospheric plasma.

ACKNOWLEDGEMENTS

EISCAT is an international association supported by research organizations in China (CRIRP), Finland (SA), France (CNRS, till end 2006), Germany (DFG), Japan (NIPR and STEL), Norway (NFR), Sweden (VR), and the United Kingdom (STFC). The data used in this paper is the property of EISCAT.

COMPETING INTERESTS

Authors have declared that no competing interests exist.

REFERENCES

1. Foster JC, del Pozo C, Groves JP, Maurice KSt. Radar observations of the onset of current driven instabilities in the topside ionosphere. Geophysical Research Letters. 1988;160-163.
2. Rietveld MT, Collis PN, St. Maurice JP. Naturally enhanced ion-acoustic waves in the auroral ionosphere observed by the EISCAT 933 MHz radar. Journal of Geophysical Research. 1991; 96,19291-19305.
3. Rietveld MT, Collis PN, Eyken AP, Løvhaug UP. Coherent echoes during EISCAT UHF common programmes. J. Atmos. Terr. Phys. 1996; Volume 58,(1),161-174.
4. Collis PN, Häggström I, Kaila K, Rietveld MT. EISCAT radar observations of enhanced incoherent scatter spectra; their relation to red aurora and field-aligned currents. Geophys. Res. Lett. 1991;18(6),1031-1034.
5. Forme FRE. A new interpretation on the origin of enhanced ion acoustic fluctuation in the upper ionosphere. Geophys. Res. Lett. 1993; 20,2347-2350.
6. Wahlund JE, Opgenoorth HJ, Forme F, Persson MAL, Häggström I, Lilensten J. Electron energization in the topside auroral ionosphere: the importance ion acoustic turbulence. J. Atm. Terr. Phys. 1993;55,623.
7. Ogawa Y, Buchert SC, Häggström I, Rietveld MT, Fujii R, Nozawa S, Miyaoka H. On the statistical relation between ion upflow and naturally enhanced ion-acoustic lines observed with the EISCAT Svalbard radar, J. Geophys. Res. 2011;116.
8. Ogawa Y, Buchert SC, Nozawa S, Forme F. Naturally enhanced ion-acoustic lines at high altitudes. Ann. Geophys. 2006; 24,3351-3364.
9. Rosenbluth MN, Rostoker N. Scattering of electromagnetic waves by a nonequilibrum plasma. Physics of Fluids. 1962; 5(7),776-788.
10. Rostoker N. Test particle method in kinetic theory of a plasma. Phys. Fluids. 1964; 7(4),491-498.
11. Trulsen J, Bjørnä N. The origin and properties of thermal fluctuations in a plasma. 1975. Institute report 17-75. The Auroral Observatory, University of Tromsø.
12. Grydeland T, Strømme A, van Eyken T, La Hoz C. The capabilities of the EISCAT Svalbard Radar for inter-hemispheric coordinated studies. Chinese J. Pol. Sci. 2002; 13(1),55-66.
13. Nygren T. Introduction to incoherent scatter measurements. 1996. Invers Publications, Invers Oy, P.O. Box 105, FIN-99601 Sodankylä, Finland, ISBN 951-97489-0-3.
14. Beynon WJG. and Williams PJS. Incoherent scatter of radio waves from the ionosphere. Rep. Prog. Phys., Vol. 41,1978.
15. Gordon WE. Incoherent scattering of radio waves by free electrons with applications to space exploration by radar. 1958; IRE,11,1824-1829, ISSN: 0096-8390.
16. Hedin M, Häggström I. Incoherent scatter spectra for non-Maxwellian plasmas. 2002, Proceedings RadioVetenskap och Kommunikation 02,RVK02,101-105.

17. Lunde J, Løvhaug UP, Gustavsson B. Particle precipitation during NEIAL events: simultaneous ground based nighttime observations at Svalbard. Ann. Geophys. 2009; 27, 2001-2010.
18. Jandieri GV and Ishimaru A. Some peculiarities of the spatial power spectrum of scattered electromagnetic waves in randomly inhomogeneous magnetized plasma with electron density and external magnetic field fluctuations. PIER B. Vol. 50, 77-95, 2013.87-100, 2012.
19. Jandieri GV, Ishimaru A, Mchedlishvili NF and Takidze IG. Spatial power spectrum of multiple scattered ordinary and extraordinarywaves in magnetized plasma with electron density fluctuations. PIER M. Vol. 25,87-100, 2012.
20. Dalipi B, Syla N. Theoretical analysis of incoherent scatter radar spectra behavior for different Maxwellian ionospheric plasma conditions. International Journal of Engineering and Technology. Vol:13 No:04,42-48, 2013.
21. Michell RG, Lynch KA, Heinselman CJ, Stenbeak-Neilsen HC. PFISR nightside observations of naturally enhanced ion acoustic lines, and their relation to boundary auroral features. Ann. Geophys. 2008; 26, 3623-3639.
22. Porteous J, Samson AM, Berrington KA, McCrea IW. Automated detection of satellite contamination in incoherent scatter radar spectra. Ann. Geophys. 2003; 21, 1177-1182.
23. Michell RG, Lynch KA, Heinselman CJ, Stenbaek-Nielsen HC. High time resolution PFISR and optical observations of naturally enhanced ion acoustic lines, Ann. Geophys. 2009; 27,1457-1467.
24. Lunde J, Gustavsson B, Løvhaug UP, Lorentzen DA, Ogawa Y. Particle precipitation during NEIAL events: simultaneous ground based observations at Svalbard. Ann. Geophys. 2007; 25,1323-1336.

Peer-review history:
The peer review history for this paper can be accessed here:
http://www.sciencedomain.org/review-history.php?iid=290&id=22&aid=2416